ARTICLE

OBC
www.rsc.org/obc

Experimental charge density of octafluoro-1,2-dimethylenecyclobutane: atomic volumes and charges in a perfluorinated hydrocarbon †

Dieter Lentz,*[a] Mona Patzschke,[a] Ansgar Bach,[b] Stephan Scheins[b] and Peter Luger*[b]

[a] *Institut für Chemie/Anorganische Chemie, Freie Universität Berlin, Fabeckstr. 34-36, D14195 Berlin, Germany*

[b] *Institut für Chemie/Kristallographie, Freie Universität Berlin, Takustr. 6, D14195 Berlin, Germany. E-mail: luger@chemie.fu-berlin.de*

Received 5th September 2002, Accepted 13th November 2002
First published as an Advance Article on the web 17th December 2002

Octafluoro-1,2-dimethylenecyclobutane, mp. 238 K, was crystallized in situ on a SMART 1000-CCD diffractometer, and high order X-ray diffraction data were collected at 100 K for a charge density determination. A topological analysis was applied and a partitioning of the molecule into atomic regions making use of Bader's zero flux surfaces yielded atomic volumes and charges. Corresponding atomic properties were also derived theoretically from B3LYP/6-311++G(3df,3pd) wavefunctions. While for carbon the volumes and charges are largely dependent on their bonding environment, fluorine has an almost constant atomic volume around 16–17 Å^3 and a charge between −0.6 and −0.7*e*, not only in the title compound, but also in two further perfluorinated hydrocarbons, of which the charge densities were determined earlier.

Introduction

The charge density $\rho(\boldsymbol{r})$ of a chemical structure can be obtained theoretically from high level *ab initio* calculations and from high-resolution X-ray diffraction experiments at low temperature.[1] Based on Bader's theory of atoms in molecules, (AIM)[2] the topological analysis of $\rho(\boldsymbol{r})$ allows a quantitative description of bonds, nonbonding interactions, electronic structure and reactivity. Moreover, a well-defined procedure of partitioning a molecule into atomic regions is provided, making use of the zero-flux surfaces (ZFS) in the electron density gradient vector field $\nabla\rho(\boldsymbol{r})$. Surfaces of this type establish atomic basins around nuclear attractors of the corresponding trajectories of $\nabla\rho(\boldsymbol{r})$. As a result, each basin uniquely defines an atomic volume. With the knowledge of the shape and volume of an atom, a number of atomic or functional group properties can be evaluated; for instance, atomic charges can be obtained by integration over the charge density in the given atomic volume.

Because of the non-trivial shape of the ZFS, they are not easy to derive and algorithms for their calculation are still very time consuming. Partitioning of experimental charge densities has become available in VALRAY[3] and very recently through the newly developed TOPXD program,[4] however, applications have been restricted mainly to smaller molecules.[5,6]

The polar C–F bond has been subject of a number of charge density studies,[6–13] however, an atomic partitioning was executed only in one case (1,1,4,4-tetrafluorobutatriene),[6] where the terminal sp^2 carbon atoms were fluorinated. Here we describe the charge density, topological bond properties and atomic volumes and charges of octafluoro-1,2-dimethylenecyclobutane (**I**), a perfluorinated hydrocarbon where fluorine is substituted to sp^2 and sp^3 carbons, as well (see Fig. 1)

Experimental

(**I**) was synthesized by thermal dimerization of tetrafluoroallene.[14] Owing to the low melting point of the title compound, crystals had to be grown in situ directly on a BRUKER SMART 1000 diffractometer, which was used for all X-ray experiments. (**I**) was condensed into a glass capillary (diameter 0.5 mm) using a glass vacuum line system on cooling with liquid nitrogen. The capillary was sealed under vacuum and brought into the cold gas stream of the diffractometer. Single crystals were grown by slow ϕ-rotation of the capillary at 237 K, very close to the melting point of (**I**). Optical inspection and the diffraction pattern seen on the area detector frames indicated that after some attempts only one single crystal was formed in the capillary.

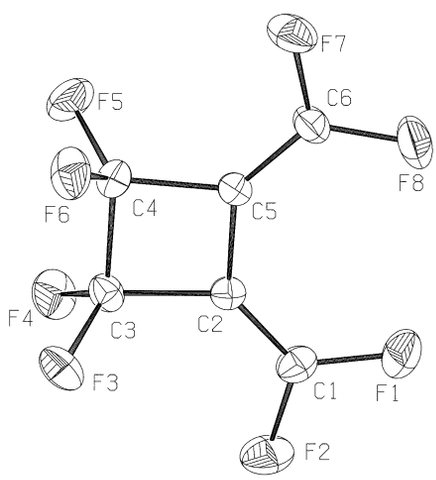

Fig. 1 ORTEP[29] representation of the molecular structure of (**I**), indicating the atom numbering scheme used. Displacement ellipsoids are drawn at a 50% probability level.

Accurate high resolution X-ray data were measured using Mo Kα-radiation (graphite monocromator). The temperature was maintained at 100 K during the measurement with an N_2-gas stream cooling device. Data were collected for two different positions of the CCD area detector. For the 2θ positions −36° and −70° a total number of 5250 frames were collected with a scan width of 0.3° in ω and an exposure time of 30 and 120 seconds, respectively. The measurement strategy was planned with ASTRO,[15] the data collection was monitored with SMART[15] and the frames were integrated with the SAINT[15]

† Electronic supplementary information (ESI) available: Crystallographic data (single crystal data) in cif format (CCDC reference number 195109), multipole population coefficients and a modified version of Table 2 containing in addition bond energies *T*, *V* and *H*. See http://www.rsc.org/suppdata/ob/b2/b208704a/

DOI: 10.1039/b208704a

Table 1 Crystal data and structure refinement for octafluoro-1,2-dimethylenecyclobutane

Empirical formula	C_6F_8
Formula weight/g mol^{-1}	224.06
Crystal system	Monoclinic
Space group	$P2_1/c$
Z	4
Temperature/K	100
Unit cell dimensions:	
a/Å	8.134(1)
b/Å	7.1110(8)
c/Å	12.699(2)
β/°	100.870(1)
V/Å^3	721.3(2)
Calculated density/g cm^{-3}	2.063
$F(000)$	432
Absorption coefficient μ/cm^{-1}	2.51
Crystal size/mm^3	Cylinder, 0.5 mm ∅
λ/Å	0.7107
$(\sin\theta/\lambda)_{max}$/Å^{-1}	1.13
Limiting indices	$-5 \le h \le 8$, $-15 \le k \le 15$, $-8 \le l \le 28$
Number of collected reflections	48515
Symmetry independent reflections	8383
Reflections with $F_o > 3\,\sigma\,(F_o)$	5127
Completeness	95.8%
Redundancy	5.3
R_{int}	0.022
N_{ref}/N_{var} [a]	26.3
R_w (multipole)	0.041
R_1 (multipole)	0.031
$R_{all}(F)$ (multipole)	0.058
Goodness of fit	2.52

[a] N_{ref}/N_{var} is the ratio between the number of reflections and the number of variables.

program. 48515 reflections were measured up to a resolution of $\sin\theta/\lambda$ = 1.13 Å^{-1} (or d = 0.44 Å) which were merged with SORTAV[16] to give 8383 unique reflections. Further details on the crystal data and the experimental conditions are given in Table 1

The structure was solved by direct methods (SHELX97),[17] followed by routine spherical refinement. The spherical model was used as input for an aspherical atom refinement with the program package XD,[18] that makes use of the Hansen–Coppens multipole formalism.[19] The hexadecapolar level of the multipolar expansion was used for all atoms. Four radial screening parameters (κ) were assigned and refined (κ_1: all F atoms, κ_2: C2 and C5, κ_3: C3 and C4, κ_4: C1 and C6). The refined κ parameters are close to 1.0 for fluorine (0.994) and show a slight contraction for carbon (κ range 1.03–1.06). In order to account for chemical symmetry and to reduce the number of variables local site symmetries and constraints were imposed. A local *mm*2 symmetry was applied to the sp^2 carbon atoms C(1) and C(6), while cylindrical symmetry was imposed on all fluorine atoms. The densities of the sp^3 fluorine atoms F(3), F(4), F(5), F(6) and of the sp^2 fluorines F(1), F(8), F(2), F(7) were constrained to be the same. This was also applied to the carbon atom pairs [C(1), C(6)], [C(2), C(5)], and [C(3), C(4)] (atomic numbering scheme see Fig. 1). The molecule was kept neutral during the refinement (neutrality constraint). In the multipole model used, a scale factor, the atomic positions, anisotropic temperature parameters of the C and F atoms, were refined together with the multipole parameters. The refinement of the 5127 unique reflections ($F_o(\boldsymbol{H}) > 3.\sigma(F_o(\boldsymbol{H}))$) yielded agreement factors of R = 3.1% and R_w = 4.1%. Experimental residual maps do not show significant residues of the electron density, no contours above 0.1e Å^{-3} are found after the multipole refinement indicating an adequate fit of the multipole model to the experimental data. Fig. 2 shows exemplarily the practically featureless residual density map in the main molecular plane.

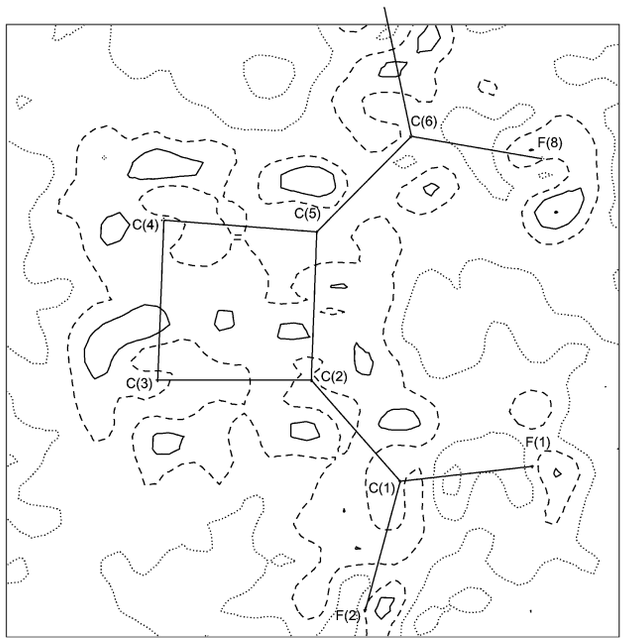

Fig. 2 Residual map in the main molecular plane. Positive, negative and zero contours are represented by solid, dotted and dashed lines, respectively. Contour intervals at 0.1e Å^{-3}.

Theoretical calculations

The GAUSSIAN98 program package[20] was used for ab initio calculations at the density functional (B3LYP) level of theory. A geometry optimization was executed for (**I**) using the 6-311++G(3df,3pd) basis set. The wave functions obtained were evalutated with the program package AIMPAC.[21]

Results and discussion

Molecular and crystal structure

The molecular structure has a main molecular plane which consists of all atoms except the fluorine substituents at C(3) and C(4). A least squares plane through the main plane atoms shows an average deviation of contributing atoms of 0.02 Å. The four atoms of the cyclobutane ring are coplanar within 0.01 Å. There is no indication for a deviation of this ring from planarity as is discussed, for example, for the X-ray structure of the free cyclobutane ring.[22]

Due to the asymmetric substitution the C–C bond lengths in the cyclobutane ring vary between 1.458(1) for the bond C(2)–C(5) between the two double bonded substituents and 1.574(1) for the bond C(3)–C(4) between the perfluorinated sp^3 carbons. In free cyclobutane the C–C bonds were uniformly found close to 1.55 Å from X-ray[22] and electron diffraction.[23] The conjugated double bonds C(1)–C(2) and C(5)–C(6) are of the same lengths as the difluorinated double bond in 1,1,4,4-tetrafluorobutadiene.[6]

The C(sp^2)-F bond lengths (average 1.308(3) Å) are, as expected, shorter than the C(sp^3)-F bonds (average 1.345(1) Å). The sp^2-C–F bonds are in the range of previous findings for this bond.[6,12,13] Also in agreement with previous findings,[12] the F–C–F angles are reduced, this holds especially for the F–C(sp^2)–F angles, which are well below 120°.

In the crystal lattice two F ··· F contacts slightly below the Bondi F ··· F van der Waals distance of 2.94 Å are seen[24] (see Fig. 3a,b). They are, however, longer than twice the major fluorine radius of 1.38 Å reported by Nyburg and Faerman.[25]

The F(2) ··· F(3) contact via the crystallographic inversion center generates a dimeric arrangement of two molecules which are linked to double layer sheets by the second contact, F(6) ··· F(8), being a pure translation in the *b*-direction (see

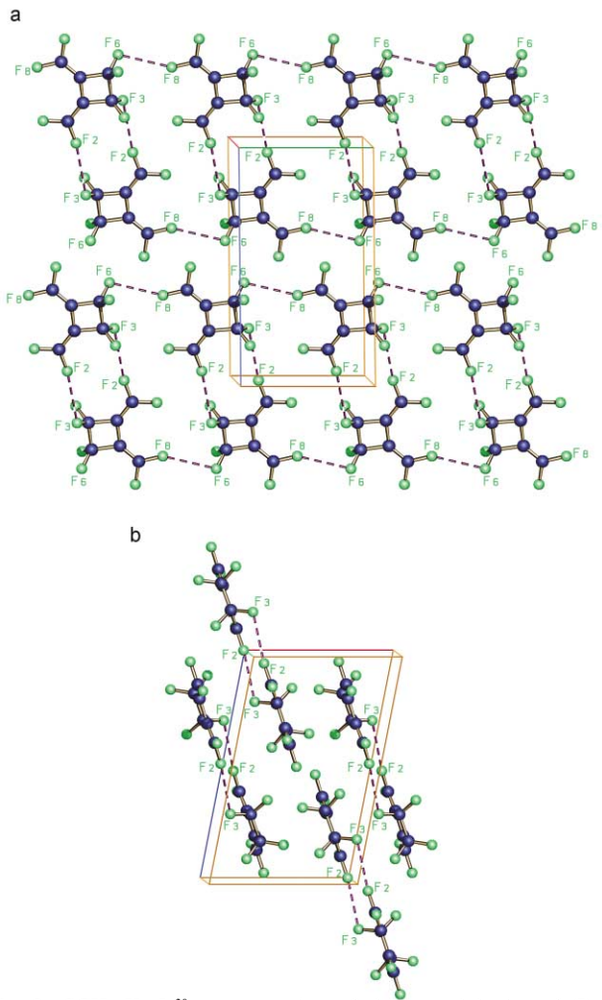

Fig. 3 SCHAKAL[30] representation of the crystal lattice of (**I**) in (a) *y*–*z*- and (b) *x*–*z*-projections. Short F ··· F contacts (F(2) ··· F(3) = 2.905(2)Å; (F(6) ··· F(8) = 2.919(3)Å) are shown by dashed lines.

Fig. 3a). These sheets form a layer structure in the crystal with the layers parallel to the ($\bar{1}$01) plane (Fig. 3b).

The average agreement in bond lengths between the experimental (multipole) geometry and the DFT optimization is better than 0.004 Å. In the theoretical model the atoms of the main molecular plane are essentially coplanar (mean deviation <0.001 Å).

Charge density and topological analysis

The experimental static deformation density $\Delta\rho(\boldsymbol{r})$ (SDD), defined as the difference between the atom-centered multipole density and the charge distribution of a hypothetical spherical promolecular density ρ(pro), was found to be in good agreement with the corresponding theoretical distribution. Only close to the fluorine nuclei, larger negative regions are seen in the theoretical distributions than experimentally. Fig. 4 compares experimental and theoretical static deformation density maps in two molecular planes. In Fig. 4a deformation density maps are shown in the main molecular plane and in Fig. 4b a plane through C(3) and its two fluorine substituents is chosen, which passes then through the diagonal of the cyclobutane ring and contains also the double bond C(5)–C(6).

On all covalent bonds and in the fluorine lone pair regions properly resolved density maxima are visible, the highest bond densities are seen on the C–C double bonds. Due to the strain in the four-membered cyclobutane ring the maxima on its bonds are shifted outward from the direct C–C vectors, illustrating the bent character of the bonds in this ring, which has already been observed in free cyclobutane.[22]

Table 2 Topological parameters at the (3,−1) bond critical points and at the (3,+1) ring critical points. First line: experimental, second line: from B3LYP calculation

Bond	Length/Å	d_1/Å[a]	$\rho(\boldsymbol{r})/e$ Å^{-3}	$\nabla^2\rho(\boldsymbol{r})/e$ Å^{-5}	ε
C(1)–F(1)	1.306(1)	0.478	2.22(4)	−27.6(3)	0.40
B3LYP	1.312	0.440	2.01	−2.7	0.17
C(1)–F(2)	1.310(1)	0.484	2.21(5)	−27.3(3)	0.40
B3LYP	1.311	0.440	2.01	−2.8	0.17
C(6)–F(7)	1.310(1)	0.484	2.21(5)	−27.3(3)	0.40
B3LYP	1.311	0.440	2.01	−2.8	0.17
C(6)–F(8)	1.304(1)	0.476	2.23(4)	−27.6(3)	0.40
B3LYP	1.312	0.440	2.01	−2.7	0.17
C(3)–F(3)	1.347(1)	0.546	2.11(5)	−20.9(2)	0.09
B3LYP	1.347	0.457	1.87	−7.1	0.15
C(3)–F(4)	1.344(1)	0.543	2.11(4)	−21.2(2)	0.06
B3LYP	1.347	0.457	1.87	−7.1	0.15
C(4)–F(5)	1.345(1)	0.544	2.11(4)	−21.1(2)	0.09
B3LYP	1.347	0.457	1.87	−7.1	0.15
C(4)–F(6)	1.345(1)	0.543	2.11(5)	−21.0(2)	0.06
B3LYP	1.347	0.457	1.87	−7.1	0.15
C(1)–C(2)	1.325(1)	0.738	2.40(4)	−26.7(2)	0.51
B3LYP	1.326	0.734	2.39	−26.9	0.51
C(5)–C(6)	1.323(1)	0.586	2.41(4)	−27.0(2)	0.51
B3LYP	1.326	0.592	2.39	−26.9	0.51
C(2)–C(5)	1.458(1)	0.730	1.85(2)	−15.79(9)	0.34
B3LYP	1.461	0.731	1.83	−16.4	0.14
C(2)–C(3)	1.509(1)	0.741	1.63(3)	−13.8(1)	0.24
B3LYP	1.515	0.746	1.76	−15.4	0.03
C(4)–C(5)	1.508(1)	0.771	1.64(3)	−13.9(1)	0.24
B3LYP	1.515	0.771	1.76	−15.4	0.03
C(3)–C(4)	1.574(1)	0.788	1.65(2)	−13.06(7)	0.13
B3LYP	1.580	0.791	1.66	−13.8	0.05
Ring 1[b]			0.41(1)	10.8(3)	
B3LYP			0.59	9.4	
Ring 2[b]			0.02(1)	0.40(1)	
B3LYP			0.03	0.6	

[a] d_1 is the distance from the bcp to the first atom given in the first column. [b] Ring 1 is the cyclobutane ring, ring 2 is the non closed ring region F(1)–C(1)–C(2)–C(5)–C(6)–F(8).

To get a quantitative description of the electronic structure of (**I**) a full topological analysis was performed with the XDPROP part of the XD program package.[18] On all covalent bonds (3,−1) bond critical points (bcp's, defined by the property that at a bcp $\boldsymbol{r}_b$ the gradient of ρ vanishes, i.e. $\nabla\rho(\boldsymbol{r}_b) = 0$) were identified. In addition two (3,+1) critical ring points were found, one in the center of the cyclobutane ring (ring 1, see Table 2) and a second one in the non closed ring region F(1)–C(1)–C(2)–C(5)–C(6)–F(8) (ring 2).

Table 2 gives a summary of quantitative experimental and theoretical topological properties at the critical points. For the nonpolar C–C bonds there is a very good agreement between the results of the experimental and theoretical topological analysis. For these bonds the $\rho(\boldsymbol{r}_b)$ values differ by 0.05e Å^{-3} (average) between experiment and theory, while the corresponding difference for the Laplacians is 0.8e Å^{-5}. As expected the strongest C–C bonds are the two conjugated double bonds with the highest $\rho(\boldsymbol{r}_b)$ values of 2.40(4) and 2.41(4)e Å^{-3}. The strain in the cyclobutane ring is also expressed by small differences between the bond path lengths and the lengths of the direct intermolecular vectors, which are 0.001–0.003 Å experimentally and 0.003–0.004 Å theoretically for the intra-ring bonds, but <0.001 Å for all other bonds.

For the polar C–F bonds the average $\rho(\boldsymbol{r}_b)$ values on the C(sp^2)–F bonds (2.22e Å^{-3}) are by 5% higher than on the C(sp^3)–F bonds (2.11e Å^{-3}). The theoretical densities at these bcp's (2.01 and 1.87e Å^{-3}) are about 90% of the experimental density, such differences were also found for the C–F bonds in pentafluorobenzoic acid (PFBA)[13] and in 1,1,4,4-tetrafluorobutatriene (TFBT).[6] The bcp-values of the Laplacians on the C–F bonds are significant different between the experimental and the theoretical model. From the experiment the Laplacians

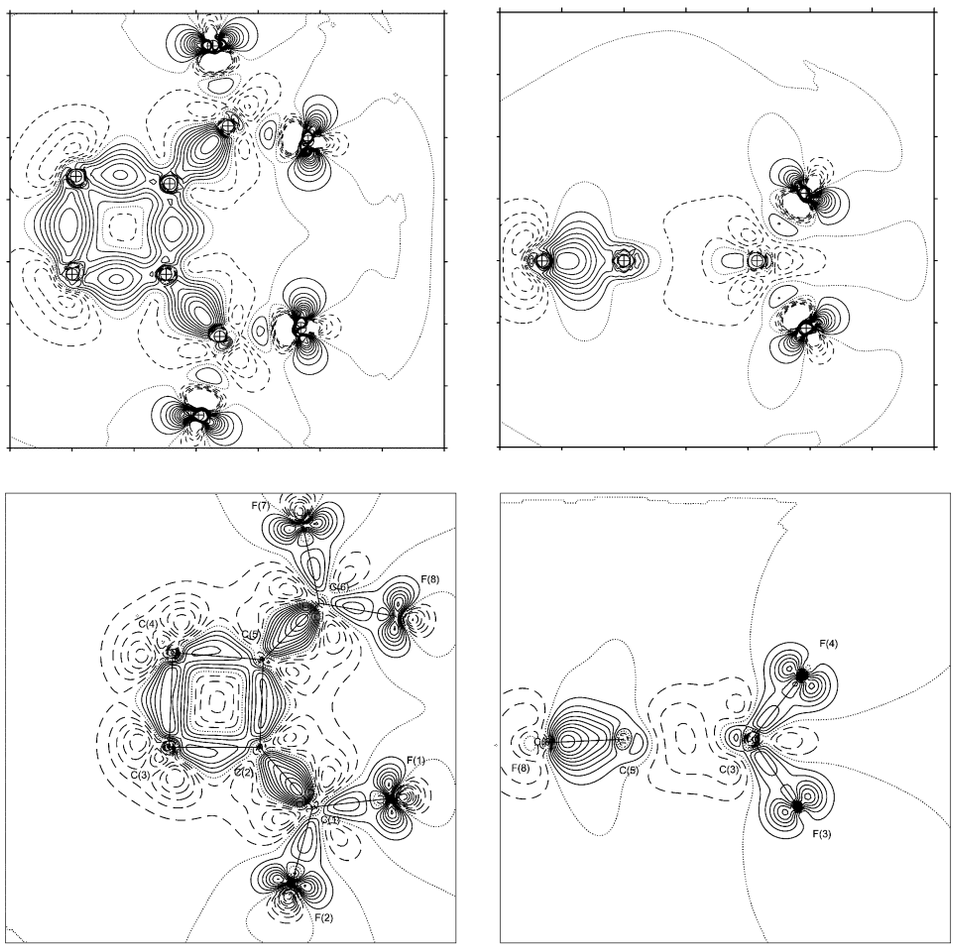

a b

Fig. 4 Theoretical (above) and static (below) deformation density maps (a) in the main molecular plane; and (b) in the plane through C(3),F(3),F(4), containing also the double bond C(5)–C(6). Contour intervals at 0.1e Å^{-3}, for further explanation see Fig. 2.

at the C–F bond critical points are in the range −21 to −28e Å^{-5}, which is typical for covalent bonds. In earlier studies $\nabla^2\rho(\boldsymbol{r}_b)$ values for C(sp^2)–F bonds were found to be −15e Å^{-5} for *p*-fluoromandelic acid,[11] −10e Å^{-5} for 1,1-difluoroallene,[12] and ranged from −18 to −26e Å^{-5} for pentafluorobenzoic acid[13] and from −24 to −25e Å^{-5} for tetrafluorobutatriene.[6] In all cases the theoretically calculated Laplacians for the C–F bond were close to zero. These differences between experiment and theory, particularly for the Laplacians at the bond critical points of polar bonds, are well known and are attributed to the nature of the radial functions in the experimental multipole model.[26]

In our earlier investigations on PFBA[13] and TFBT[6] we have studied the detailed distribution of $\rho(\boldsymbol{r})$ and $\nabla^2\rho(\boldsymbol{r})$ on a C–F bond, where it was shown that, in contrast to a C–C bond, $\nabla^2\rho(\boldsymbol{r})$ is positive between the nuclei except for a narrow range around the valence shell charge concentration of the carbon atom and changes from negative to positive close to the bcp. Since the location of the bcp can differ by ~0.05–0.1 Å between experiment and theory (see the column for d_1 in Table 2), this small shift in the bcp can lead to the found differences in the $\nabla^2\rho(\boldsymbol{r}_b)$ values.

The electrostatic potential, which was calculated using the method of Su and Coppens[27] on the basis of the experimental charge density, is displayed as an isosurface representation in Fig. 5. As expected, the negative potential is concentrated around the fluorine atoms, while the cyclobutane ring region is positive. In total the molecule is surrounded by a shell of negative potential, so that it makes sense that no closer intermolecular approach than the above mentioned F ··· F contact next to the van der Waals distances exists.

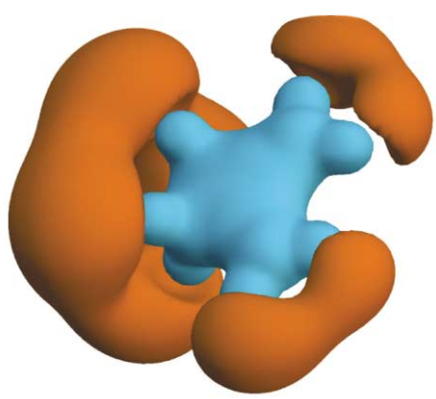

Fig. 5 Three-dimensional representation of the electrostatic potential based on the experimental charge density: Two isopotential surfaces are shown: blue: 0.5, red: −0.02e Å^{-1}.

Atomic volumes and charges

For the evaluation of atomic volumes and charges after Bader's definition from the X-ray charge density, the algorithm available through TOPXD[4] was applied. Comparison was made then with the corresponding theoretical quantities which were extracted from DFT densities with MORPHY.[28] To allow a wider comparison of fluorine atomic properties bonded to hydrocarbons we included also PFBA in the partitioning calculations, making use of its experimental charge density we had published earlier.[13]

An illustration of the experimental gradient vector field $\nabla\rho(\vec{\boldsymbol{r}})$ in the main molecular plane is shown in Fig. 6, while the

Table 3 Summary of atomic volumes/Å^3 and charges/*e* in the title compound (**I**) and for comparison in PFBA

Atom	V_{tot} (exp)	V_{001} (exp) Charge (exp)	V_{001} (DFT) Charge (DFT)
C1	6.99	6.88	7.39
		1.22	1.21
C6	6.61	6.61	7.37
		1.23	1.21
C2	10.11	9.79	10.51
		0.40	0.10
C5	10.11	9.84	10.49
		0.40	0.10
C3	4.09	4.09	4.41
		1.37	1.26
C4	4.06	4.06	4.41
		1.38	1.26
F1	17.35	16.51	15.73
		−0.77	−0.64
F2	17.68	16.38	15.86
		−0.76	−0.64
F7	16.79	15.96	15.85
		−0.76	−0.64
F8	18.47	16.52	15.73
		−0.77	−0.64
F3	15.64	15.15	15.70
		−0.73	−0.64
F4	17.70	15.73	15.70
		−0.74	−0.64
F5	17.09	15.44	15.69
		−0.73	−0.64
F6	17.35	15.73	15.69
		−0.74	−0.64
Σ vol	180.04	168.69	170.53
Σ charge		0.0	0.02
PFBA			
Average C_{ph}	8.45(42)	8.18(34)	8.65(8)
(C2–C6)		0.64(10)	0.63(1)
Average F	15.89(68)	14.72(24)	15.64(12)
(F2–F6)		−0.65	−0.64(1)
C1	9.54	9.51	10.32
		0.20	0.04
C7	5.53	5.50	5.29
		1.41	1.64
O1	17.16	16.36	19.67
		−1.23	−1.14
O2	17.24	15.48	17.51
		−1.00	−1.12
H1	1.25	1.23	3.11
		0.68	0.61

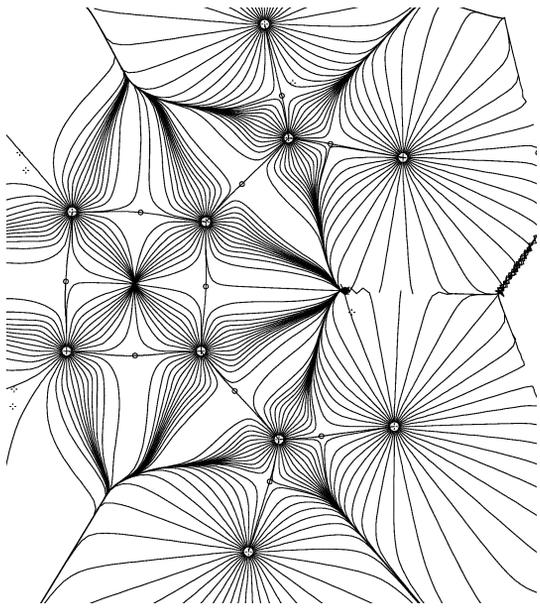

Fig. 6 Gradient vector field $\nabla\rho(\boldsymbol{r})$ in the main molecular plane of (**I**).

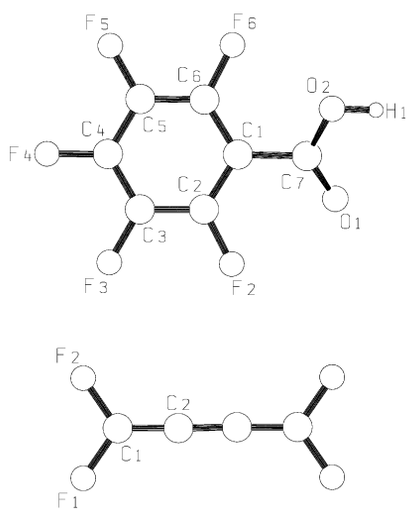

Fig. 7 Molecular structures and atomic numbering scheme for pentafluorobenzoic acid (PFBA)[13] and 1,2,4,4-tetrafluorobutatriene (TFBT).[6]

numerical results are summarized in Table 3. The theoretical volumes, denoted V_{001}, are based on a cutoff ρ = 0.001 au, which is commonly used in theory. This cutoff was also used for the experimental densities V_{001} (see corresponding column in Table 3) which are given in addition to the volumes defined by the interatomic boundaries in the crystal (column V_{tot}) to allow for an adequate comparison between experiment and theory. The sum of the V_{tot} volumes (multiplied by Z = 4) reproduces the unit cell volume to within 1.1 Å.^{3} If experimental and DFT atomic volumes are compared, it can be seen that for the carbon atoms the DFT volumes are by 8–12% larger than both the V_{tot} and V_{001} volumes, whereby the latter do not differ too much. The opposite is seen for the fluorine volumes, however, for these atoms V_{tot} (exp) is larger, but the remarkably smaller experimental V_{001} volumes agree very closely with the theoretical ones. This is also indicated by the molecular V_{001} volumes, which agree within 2 Å^3 for experiment and theory.

In line with their chemical environment the carbon atom volumes group into three types. The sp^2 carbons C(2) and C(5) lacking fluorine substituents are the largest ones while C(1) and C(6), carrying two fluorines each, have a strongly reduced volume. Further volume reduction is seen for the difluorinated sp^3 carbons C(3) and C(4). These findings, which are supported by the theoretically obtained volumes, agree with the corresponding results for PFBA. In this molecule (see molecular structure and atomic numbering scheme in Fig. 7) the only non-fluorosubstituted carbon atom in the phenyl ring is C1, having a volume close to 10 Å^3 as C2 and C5 in the title compound. The other monofluorinated phenyl carbons have volumes around 8.6 Å^3, which are between non- and difluorosubstituted sp^2 carbons. Hence with increasing substitution the carbons lose volume, which is taken by the electronegative fluorines. For the fluorine atoms, their volume is obviously independent of whether they are bonded to an sp^2 or an sp^3 carbon. This tendency is seen for the experimental and theoretical volumes for the title compound. For PFBA the experimental volumes are ~1 Å^3 smaller, while the theoretical volumes closely agree. Also the two fluorines in TFBT (Fig. 7) have volumes[6] very close to 16 Å^3, so that in all cases Bader volumes for fluorine are constantly found at 16–17 Å^3.

Very uniform are also the fluorine atom charges. While the experimentally obtained fluorine atomic charges differ by 4% whether they are bonded to sp^2 or sp^3 carbons, with the latter the slightly smaller ones, the DFT derived charges are surprisingly constant at −0.64*e*. For the five fluorines substituted to the phenyl ring in PFBA their charges were found to be

$-0.65/-0.64e$ (experiment/theory). The corresponding quantities in TFBT were $-0.59/-0.64e$.

The strong negative charges of the electronegative fluorines are compensated by high positive charges at the carbons, which are highest at C(3) and C(4) corresponding to the smallest volume. This tendency is supported by the results from DFT, however, in theory, the ring atoms C(2) and C(5) are practically neutral. In PFBA the negative and positive charges of F and C cancel out, so that in total the perfluorinated phenyl ring is almost neutral.

Conclusion

As far as we know, the perfluorinated title compound is the first one, where topological bond descriptors, atomic volumes and charges could be studied for fluorine substituted to both sp^3 and sp^2 carbons. Although the bond lengths are different by 0.04 Å, the topological properties show minor differences. This holds for the charge densities on the bond critical points and even more uniform for atomic properties. Fluorine exhibits an almost constant volume of 16–17 $Å^3$ in the title compound, in PFBA and also in the $R{=}CF_2$ fragment of TFBT. Also the AIM charge of fluorine is conserved. In all fluorine compounds where AIM charges have been evaluated so far, fluorine atoms carry a negative charge of around $-0.7e$ with a spread of less than $0.1e$ (experiment), while DFT theory gives uniformly $-0.64e$. The topological analyses carried out until now on fluorinated hydrocarbon charge densities indicate therefore a high transferability of fluorine electronic properties.

Acknowledgements

We thank the Deutsche Forschungsgemeinschaft, DFG (grant Lu222/18–3) and the Fonds der Chemischen Industrie for financial support.

References

1 P. Coppens, *X-Ray Charge Densities and Chemical Bonding*, Oxford University Press, New York, 1997; T.S. Koritsanszky and P. Coppens, *Chem. Rev.*, 2001, **101**, 1583.
2 R. F. W. Bader, *Atoms in Molecules*, Clarendon Press, Oxford, 1994; R. F. W. Bader in *The Encyclopedia of Computational Chemistry*, ed. P. von R. Schleyer, N. L. Allinger, T. Clark, J. Gasteiger, P. A. Kollman, H. F. Schaefer III and P. R. Schreiner, Wiley, Chichester, 1998.
3 R. F. Stewart, M. A. Spackman, *VALRAY User's Manual*; Carnegie-Mellon University: Pittsburgh, PA, 1983; C. Flensburg and D. Madsen, *Acta Crystallogr. A*, 2000, **56**, 24.
4 TOPXD: A. Volkov, C. Gatti, Y. Abramov and P. Coppens, *Acta Crystallogr., Sect. A*, 2000, **A56**, 252.
5 M. Messerschmidt, A. Wagner, M.W. Wong and P. Luger, *J. Am. Chem. Soc.*, 2002, **124**, 732.
6 A. Bach, D. Lentz, P. Luger, M. Messerschmidt, Ch. Olesch and M. Patzschke, *Angew. Chem.*, 2002, **114**, 311 (*Angew. Chem., Int. Ed.*, 2002, **41**, 296).
7 J. Buschmann, T. Koritsanszky, R. Kuschel, P. Luger and K. Seppelt, *J. Am. Chem. Soc.*, 1991, **113**, 233.
8 M. Kubota and S. Ohba, *Acta Crystallogr., Sect. B*, 1992, **B48**, 849.
9 H. Irngartinger and S. Shack, *J. Am. Chem. Soc.*, 1998, **120**, 5818.
10 P. R. Mallinson, G. Barr, S. J. Coles, T. N. Guru Row, D. D. McNicol, S. J. Teat and K. Wozniak, *J. Synchrotron Radiat.*, 2000, **7**, 160.
11 S. Larsen, C. Flensburg, H. S. Bengacted and H. O. Sorenson, *Acta Crystallogr., Sect. A*, 1999, **A55**, 38.
12 J. Buschmann, T. Koritsanszky, D. Lentz, P. Luger, N. Nickelt and S. Willemsen, *Z. Kristallogr.*, 2000, **215**, 487.
13 A. Bach, D. Lentz and P. Luger, *J. Phys. Chem A*, 2001, **105**, 7405.
14 T. L. Jacob and R.S. Bauer, *J. Am. Chem. Soc.*, 1959, **81**, 606.
15 Programs ASTRO (1995–1996), SMART (1996), SAINT (1994–1996), SORTAV, Bruker-AXS Inc., Madison, WI.
16 R. H. Blessing, *Acta Crystallogr. A*, 1995, **51**, 33–38.
17 G. M. Sheldrick SHELX97 Programs for Crystal Structure Analysis (Release 97–2), University of Göttingen, Germany, 1998.
18 T. Koritsanszky, S. Howard, P. R. Mallinson, Z. Su, T. Richter and N. K. Hansen, *XD – a Computer Program Package for Multipole Refinement and Analysis of Electron Densities from Diffraction Data, User manual*, Freie Universität Berlin, Germany, 1995.
19 N. K. Hansen and P. Coppens, *Acta Crystallogr., Sect. A*, 1978, **A34**, 909.
20 M. J. Frisch, G. W. Trucks, H. B. Schlegel, G. E. Scuseria, M. A. Robb, J. R. Cheeseman, V. G. Zakrzewski, J. A. Montgomery, Jr., R. E. Stratmann, J. C. Burant, S. Dapprich, J. M. Millam, A. D. Daniels, K. N. Kudin, M. C. Strain, O. Farkas, J. Tomasi, V. Barone, M. Cossi, R. Cammi, B. Mennucci, C. Pomelli, C. Adamo, S. Clifford, J. Ochterski, G. A. Petersson, P. Y. Ayala, Q. Cui, K. Morokuma, P. Salvador, J. J. Dannenberg, D. K. Malick, A. D. Rabuck, K. Raghavachari, J. B. Foresman, J. Cioslowski, J. V. Ortiz, A. G. Baboul, B. B. Stefanov, G. Liu, A. Liashenko, P. Piskorz, I. Komaromi, R. Gomperts, R. L. Martin, D. J. Fox, T. Keith, M. A. Al-Laham, C. Y. Peng, A. Nanayakkara, M. Challacombe, P. M. W. Gill, B. G. Johnson, W. Chen, M. W. Wong, J. L. Andres, C. Gonzalez, M. Head-Gordon, E. S. Replogle and J. A. Pople, GAUSSIAN 98 (Revision A.7), Gaussian, Inc., Pittsburgh, PA, 1998.
21 J. Cheeseman, T. A. Keith and R. F. W. Bader, AIMPAC program package, McMaster University, Hamilton, ON, 1992.
22 A. Stein, Ch. W. Lehmann and P. Luger, *J. Am. Chem. Soc.*, 1992, **114**, 7684.
23 A. Almenningen, O. Bastiansen and P. N. Skancke, *Acta Chem. Scand.*, 1961, **15**, 711.
24 A. Bondi, *J. Phys. Chem.*, 1964, **68**, 441.
25 S. C. Nyburg and H. Faerman, *Acta Crystallogr., Sect. B*, 1985, **B41**, 274.
26 A. Volkov, Y. Abramov, P. Coppens and C. Gatti, *Acta Crystallogr., Sect. A*, 2000, **A56**, 332.
27 Z. W. Su and P. Coppens, *Acta Crystallogr., Sect. A*, 1992, **A48**, 188.
28 P. L. A. Popelier, *MORPHY98*, University of Manchester Institute of Science and Technology, UK, 1998, with a contribution from R. G. A. Bone.
29 M. N. Burnett and C. K. Johnson, ORTEP-III, Oak Ridge Thermal Ellipsoid Plotting Program for Crystal Structure Illustrations, ORNL-6895, Oak Ridge National Laboratory, Oak Ridge, TN, 1996.
30 E. Keller, SCHAKAL88. A Fortran Program for the Graphical Representation of Molecular and Crystallographic Models, University of Freiburg, Germany, 1988.